

BIFURCATIONS OF PERIODIC SOLUTIONS AND CHAOS IN DUFFING-VAN DER POL EQUATION WITH ONE EXTERNAL FORCING*

Zhiyan Yang¹, Tao Jiang^{1,†} and Zhujun Jing²

Abstract The Duffing-Van der Pol equation with fifth nonlinear-restoring force and one external forcing term is investigated in detail: the existence and bifurcations of harmonic and second-order subharmonic, and third-order subharmonic, third-order superharmonic and m -order subharmonic under small perturbations are obtained by using second-order averaging method and subharmonic Melnikov function; the threshold values of existence of chaotic motion are obtained by using Melnikov method. The numerical simulation results including the influences of periodic and quasi-periodic and all parameters exhibit more new complex dynamical behaviors. We show that the reverse period-doubling bifurcation to chaos, period-doubling bifurcation to chaos, quasi-periodic orbits route to chaos, onset of chaos, and chaos suddenly disappearing, and chaos suddenly converting to period orbits, different chaotic regions with a great abundance of periodic windows (periods: 1, 2, 3, 4, 5, 7, 9, 10, 13, 15, 17, 19, 21, 25, 29, 31, 37, 41, and so on), and more wide period-one window, and varied chaotic attractors including small size and maximum Lyapunov exponent approximate to zero but positive, and the symmetry-breaking of periodic orbits. In particular, the system can leave chaotic region to periodic motion by adjusting the parameters p, β, γ, f and ω , which can be considered as a control strategy.

Keywords Duffing-Van der Pol equation, bifurcations, periodic solutions, chaotic attractors, complex period windows.

MSC(2000) 37G15, 37D45.

1. Introduction

In this paper, we consider the following Duffing-Van der Pol (DVP) equation with fifth nonlinear force and one external forcing

$$\ddot{x} + p(x^2 - 1)\dot{x} + \omega_0^2 x + \beta x^3 + \gamma x^5 = f \cos \omega t, \quad (1.1)$$

[†]the corresponding author. Email address: taojiang@amss.ac.cn (T. Jiang)

¹The Information School, Beijing Wuzi University, 101149 Beijing, China

²The center for Dynamical systems, Academy of Mathematical and system sciences, Chinese Academy of Sciences, Beijing, 100080, China

*The authors were supported by the National Science Foundations of China (10671063 and 10801135) and the Special Fund of Ministry of Education of Beijing and Youth Fund of Beijing Wuzi University.

where $p, \omega_0, \beta, \gamma, f, \omega$ are real parameters. Physically, p can be regarded as dissipation or damping, β and γ are the strength of nonlinearity, f and ω as the amplitude and frequency of the external force.

The Duffing equation (i.e., $p = 0$ in (1.1)) and Van der Pol equation (i.e., $\beta = 0, \gamma = 0$ in (1.1)) have been extensively studied from analytical and numerical investigations. The bifurcations of periodic solution, bifurcation structures and chaotic behaviors with complex period windows are shown in [2, 5, 6, 10, 22, 25].

The Duffing-Van der Pol equation is a combination of Duffing and Van der Pol equations and has application in the simulation of nonlinear oscillation systems [9, 20]. The dynamical behaviors of the Duffing-Van der Pol equation as the parameters varying are considered in [8, 14, 15, 19]. In the previously work [7], we investigate the Duffing-Van der Pol equation with two external forcings, and give the threshold values of existence of chaos under the periodic perturbation, and the criterion of existence of chaos in averaged system under quasi-periodic perturbation for $\omega_2 = n\omega_1 + \epsilon\sigma$, $n = 1, 3, 5$, and can't prove the criterion of existence of chaos in second-order averaged system under quasi-periodic perturbation for $\omega_2 = n\omega_1 + \epsilon\sigma$, $n = 2, 4, 6, 7, 8, 9, 10$, where σ is not rational to ω_1 , and obtain rich dynamical behaviors by numerical simulations. In this paper, the bifurcations of periodic orbits, and chaos for (1.1) are investigated by using second-order averaging method and Melnikov methods in [1, 3–5, 11–13, 16–18, 21, 23, 24]. We give the existence and bifurcations of harmonics and second-order subharmonic, and third-order subharmonic, third-order superharmonic and m -order subharmonic under small perturbations, and the criterion of existence of chaos. We also give numerical simulations including bifurcation diagrams of fixed points and system, computation of maximum Lyapunov exponents, phase portraits, and Poincaré map, and consider the influences of periodic and quasi-periodic and all parameters. We show that the reverse period-doubling bifurcation to chaos, period-doubling bifurcation to chaos, quasi-period route to chaos, onset of chaos, and chaos suddenly disappearing and chaos suddenly converting to period orbits, different chaotic regions with a great abundance of periodic windows (periods: 1, 2, 3, 4, 5, 7, 9, 10, 13, 15, 17, 19, 21, 25, 29, 31, 37, 41, and so on), and more wide period-one window, and varied chaotic attractors including small size and maximum Lyapunov exponent approximate to zero but positive, and the symmetry-breaking of periodic orbits. In particular, the system can leave chaotic region to periodic motion by adjusting the parameters p, β, γ, f and ω , which can be considered as a control strategy.

The paper is organized as follows. Analytical results for the conditions of existence and bifurcations of harmonic and second-order subharmonics are given in section 2 and 3, respectively. In section 4, we provide the conditions of existence and bifurcation for the third-order subharmonic resonance. In section 5, the criterion for the existence of m -order subharmonics is proved by using subharmonic Melnikov function. In section 6, we present the conditions of existence and bifurcation for the third-order superharmonic resonance. In section 7, Melnikov's method is used to prove the existences of homoclinic bifurcation and heteroclinic bifurcation. The numerical simulations including bifurcation diagrams in $(x - f)$, $(x - \omega_0)$, $(x - \gamma)$, $(x - \beta)$, $(x - p)$, and $(x - \omega)$ planes, the computation of maximum Lyapunov exponent corresponding to bifurcation diagram, the phase portrait and Poincaré map at neighborhood of critical values, are given in section 8. Finally, we give remark in section 9.

2. Primary Resonance and Bifurcation

In this section, we consider primary resonance using the second-order averaging method. Introduce a small parameter ϵ , such that $0 < \epsilon \ll 1$ and replace p and f by ϵp and $\epsilon^{\frac{3}{2}} f$ respectively, then (1.1) can be rewritten as

$$\begin{cases} \dot{x} = y, \\ \dot{y} = -\omega_0^2 x - \beta x^3 - \gamma x^5 - \epsilon p(x^2 - 1)y + \epsilon^{\frac{3}{2}} f \cos \omega t. \end{cases} \quad (2.1)$$

Let $(x_0, 0)$ be a center of (2.1) for $\epsilon = 0$ and the frequency of periodic orbit near the center is approximately given by

$$a_1 = \sqrt{\omega_0^2 + 3\beta x_0^2 + 5\gamma x_0^4}. \quad (2.2)$$

If the ratio of ω and a_1 is a rational number, then the resonance behavior may occur in (2.1). We now consider the case of primary resonance $\omega \approx a_1$ for (2.1). Assume that

$$\omega^2 \approx a_1^2, \quad \epsilon \Omega = \omega^2 - a_1^2. \quad (2.3)$$

Let

$$a_2 = 3\beta x_0 + 10\gamma x_0^3, \quad a_3 = -\beta - 10\gamma x_0^2, \quad \alpha = x_0^2 - 1, \quad x = x_0 + \sqrt{\epsilon}z. \quad (2.4)$$

Then (2.1) can be rewritten as

$$\ddot{z} + a_1^2 z = -\sqrt{\epsilon} a_2 z^2 + \epsilon(a_3 z^3 - p\alpha \dot{z} + f \cos \omega t) + O(\epsilon^{\frac{3}{2}}). \quad (2.5)$$

We use the Van der Pol transformation

$$\begin{pmatrix} u \\ v \end{pmatrix} = \begin{pmatrix} \cos \omega t & -\frac{1}{\omega} \sin \omega t \\ -\sin \omega t & -\frac{1}{\omega} \cos \omega t \end{pmatrix} \begin{pmatrix} z \\ \dot{z} \end{pmatrix}, \quad (2.6)$$

and carry out averaging up to second-order for (2.5). We obtain the following averaged equation

$$\begin{aligned} \dot{u} &= \frac{\epsilon}{2a_1} (\Omega v - p\alpha a_1 u + b_0 v(u^2 + v^2)), \\ \dot{v} &= \frac{\epsilon}{2a_1} (-\Omega u - p\alpha a_1 v - b_0 u(u^2 + v^2) - f), \end{aligned} \quad (2.7)$$

where $b_0 = \frac{9a_1^2 a_3 + 10a_2^2}{12a_1^2}$.

In polar coordinates $r = \sqrt{u^2 + v^2}$ and $\theta = \arctan(v/u)$, (2.7) becomes

$$\begin{aligned} \dot{r} &= \frac{\epsilon}{2a_1} (-p\alpha a_1 r - f \sin \theta), \\ r\dot{\theta} &= \frac{\epsilon}{2a_1} (-\Omega r - b_0 r^3 - f \cos \theta). \end{aligned} \quad (2.8)$$

The fixed points of (2.8) satisfy the following equation

$$b_0^2 y^3 + 2b_0 \Omega y^2 + (p^2 \alpha^2 a_1^2 + \Omega^2) y = f^2, \quad (2.9)$$

where $y = r^2$. Let

$$F_0(y) = b_0^2 y^3 + 2b_0 \Omega y^2 + (p^2 \alpha^2 a_1^2 + \Omega^2) y - f^2, \quad (2.10)$$

and $y = x - \frac{2\Omega}{3b_0}$, then (2.9) becomes

$$x^3 + sx + q = 0, \tag{2.11}$$

where $s = \frac{3p^2\alpha^2 a_1^2 - \Omega^2}{3b_0^2}$, $q = \frac{-2\Omega^3}{27b_0^3} - \frac{2\Omega p^2\alpha^2 a_1^2}{3b_0^3} - \frac{f^2}{b_0^2}$.

The discriminant of (2.11) is given by

$$\begin{aligned} \Delta &= \left(\frac{q}{2}\right)^2 + \left(\frac{s}{3}\right)^3 \\ &= \frac{f^4}{4b_0^4} + \frac{\Omega}{27b_0^5}(\Omega^2 + 9p^2\alpha^2 a_1^2)f^2 + \frac{p^2\alpha^2 a_1^2}{27b_0^6}(\Omega^2 + p^2\alpha^2 a_1^2)^2. \end{aligned} \tag{2.12}$$

Let

$$\Delta = 0, \tag{2.13}$$

and Δ' denotes the discriminant of (2.13), then $\Delta' = \frac{16}{27b_0^6}(\Omega^2 - 3p^2\alpha^2 a_1^2)^3$. We have the following conclusion as $b_0\Omega < 0$.

(i) If $\Delta' > 0$, then there exist two real roots of (2.13) as following

$$f_1^2 = \frac{1}{27b_0}(-2\Omega(\Omega^2 + 9p^2\alpha^2 a_1^2) - 2(\Omega^2 - 3p^2\alpha^2 a_1^2)\sqrt{\Omega^2 - 3p^2\alpha^2 a_1^2}), \tag{2.14}$$

and

$$f_2^2 = \frac{1}{27b_0}(-2\Omega(\Omega^2 + 9p^2\alpha^2 a_1^2) + 2(\Omega^2 - 3p^2\alpha^2 a_1^2)\sqrt{\Omega^2 - 3p^2\alpha^2 a_1^2}). \tag{2.15}$$

(ii) If $\Delta' < 0$, then there exists not any real root of (2.13).

(iii) If $\Delta' = 0$, then there exists one root of (2.13), that is $f^2 = \left|\frac{8\sqrt{3}p^3\alpha^3 a_1^3}{9b_0}\right|$.

For $b_0\Omega > 0$, Δ is always positive.

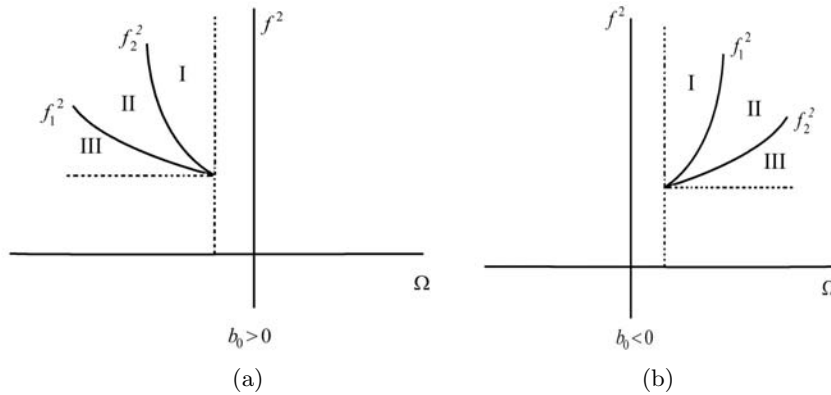


Figure 1. Super-critical and sub-critical saddle-node bifurcation curves: (a) $b_0 > 0$; (b) $b_0 < 0$.

In Fig.1 we have drawn the bifurcation curves f_1^2 and f_2^2 in the (Ω, f) -plane and Fig1.(a) and Fig1.(b) correspond to $b_0 > 0$ and $b_0 < 0$, respectively. The plane in Fig.1 is divided into three regions (I), (II), (III) by the two branches f_1^2 and f_2^2 , which meet at $(\Omega_{1,2}, f) = (\pm\sqrt{3}p\alpha a_1, \sqrt{|\frac{8\sqrt{3}(p\alpha a_1)^3}{9b_0}}|)$.

By the above analysis we have the following lemma:

Lemma 2.1. (i) If (Ω, f^2) lies in (I) and (III), there exist one real root of (2.9) which corresponds to one nontrivial fixed point of (2.8); if (Ω, f^2) lies in (II), there exist three distinct real roots of (2.9) which correspond to three distinct nontrivial fixed points of (2.8).

(ii) If (Ω, f^2) lies in the curve f_1^2 or f_2^2 , there are three real roots of (2.9), but two of them coincide; on f_1^2 the coincidence occurs for the root $y = \frac{-2\Omega + \sqrt{\Omega^2 - 3p^2\alpha^2 a_1^2}}{3b_0}$; on f_2^2 for the root $y = \frac{-2\Omega - \sqrt{\Omega^2 - 3p^2\alpha^2 a_1^2}}{3b_0}$, which corresponds to two nontrivial fixed points of (2.8).

(iii) If (Ω, f^2) lies at the point $(\pm\sqrt{3p\alpha a_1}, \sqrt{|\frac{8\sqrt{3}(p\alpha a_1)^3}{9b_0}|})$, there are three coincident real roots, which correspond to one nontrivial fixed point of (2.8).

(v) If $b_0\omega > 0$ or $\Omega^2 \leq 3p^2\alpha^2 a_1^2$, there is one real root of (2.9), which corresponds to one nontrivial fixed point of (2.8).

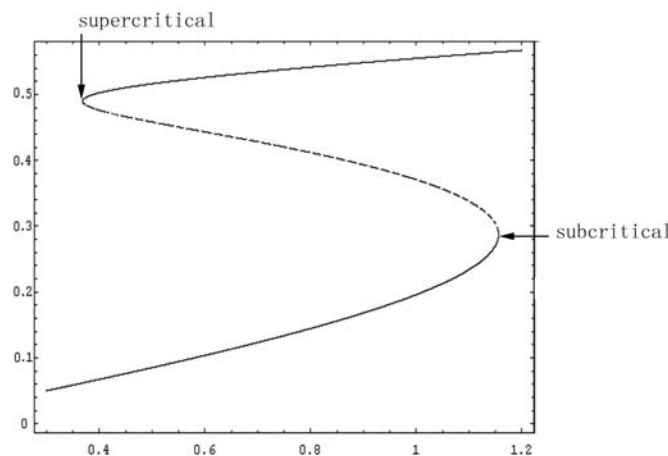


Figure 2. A bifurcation diagram. Here $\beta = -2, \gamma = 0.5, \omega_0 = 1, p = 0.1, \Omega = -6, a_1 = 3.10755, b_0 = 24.8088, \alpha = 2.41442$.

The stability of fixed point (r_s, θ_s) of (2.8) is determined by the characteristic values

$$\lambda_{1,2} = -p\alpha a_1 \pm \sqrt{p^2\alpha^2 a_1^2 - F'_0(y_s)}, \tag{2.16}$$

where $y_s = r_s^2$ and $F'_0(y_s) = 3b_0^2 y_s^2 + 4b_0\Omega y_s + \Omega^2 + p^2\alpha^2 a_1^2$.

Furthermore, we know that the averaged system (2.8) (or (2.7)) has no closed orbit by the Dulac's criterion.

Thus, by considering the above stability conditions and Lemma 2.1, we can get the following conclusion for $\alpha > 0$:

Lemma 2.2. (i) For $b_0\Omega > 0$ and $0 < \epsilon \ll 1$, there exists one stable foci-node.

(ii) For $\Omega^2 - 3p^2\alpha^2 a_1^2 > 0, b_0\Omega < 0$ and $0 < \epsilon \ll 1$, there exist two stable foci-node and one saddle in region (II); there exists a stable foci-node in region (I) and (III). On the curves f_1^2 and f_2^2 there is one stable foci-node and a fixed point which has one zero eigenvalue.

- (iii) For $\Omega^2 - 3p^2\alpha^2a_1^2 \leq 0$, $b_0\Omega < 0$ and $0 < \epsilon \ll 1$, there exists a stable foci-node except the point $(\Omega, f) = (\pm\sqrt{3p\alpha a_1}, \sqrt{|\frac{8\sqrt{3}(p\alpha a_1)^3}{9b_0}|})$ at which there is a fixed point with one zero eigenvalue.
- (iv) When f^2 increases, the fixed point changes from one to three, passing through f_2^2 for $b_0 < 0$ or f_1^2 for $b_0 > 0$; on f_2^2 or f_1^2 , there are two fixed points and one of them has a zero eigenvalue, so f_2^2 or f_1^2 is supercritical saddle-node bifurcation. When f^2 decreases, the fixed point changes from one to three, passing through f_1^2 for $b_0 < 0$ or f_2^2 for $b_0 > 0$; on f_1^2 or f_2^2 , there are two fixed points and one of them has a zero eigenvalue, so f_1^2 or f_2^2 is subcritical saddle-node bifurcation.

Fig.2 shows a bifurcation diagram indicating how the fixed points of (2.8) are created or annihilated when f is varying while the other parameters remain fixed.

For $\alpha < 0$, the stable foci-node becomes unstable and the stability of other fixed points does not change in Lemma 2.2.

Thence, we can give the following theorem by the averaging theorem ([5,21,24]).

Theorem 2.1. For (2.1), we have:

- (i) For $b_0\Omega > 0$ and $0 < \epsilon \ll 1$, there exists a stable resonant harmonic solution for $\alpha > 0$ and an unstable resonant harmonic solution for $\alpha < 0$.
- (ii) For $b_0\Omega < 0$, $\Omega^2 - 3p^2\alpha^2a_1^2 > 0$, and $0 < \epsilon \ll 1$, there exist two stable resonant harmonic solutions for $\alpha > 0$ and two unstable resonant harmonic solutions for $\alpha < 0$ and one unstable resonant harmonic solution in region (II); there is a stable resonant harmonic solution for $\alpha > 0$ and an unstable resonant harmonic solution for $\alpha < 0$ in regions (I) and (III). When $\alpha > 0$, a stable harmonic appears near the supercritical bifurcation curve f_2^2 or f_1^2 and a stable harmonic disappears near the subcritical bifurcation curve f_1^2 or f_2^2 for $b_0 > 0$ or $b_0 < 0$, respectively. When $\alpha < 0$, an unstable harmonic appears near the supercritical bifurcation curve f_2^2 or f_1^2 and an unstable harmonic disappears near the subcritical bifurcation curve f_1^2 or f_2^2 for $b_0 > 0$ or $b_0 < 0$, respectively.
- (iii) For $\Omega^2 - 3p^2\alpha^2a_1^2 \leq 0$, $b_0\Omega < 0$ and $0 < \epsilon \ll 1$, there exists a stable harmonic solution for $\alpha > 0$ and an unstable harmonic solution for $\alpha < 0$. At the point $(\Omega, f) = (\pm\sqrt{3p\alpha a_1}, \sqrt{|\frac{8\sqrt{3}(p\alpha a_1)^3}{9b_0}|})$, there also exists a harmonic solution.
- (iv) The harmonic solution of (2.1) is approximately given by

$$x(t) = x_0 + \sqrt{\epsilon}r_s \cos(\omega t + \theta_s) + O(\epsilon),$$

where (r_s, θ_s) is given by the equilibrium solution of averaged (2.8). The other solutions in (2.8) correspond to the almost periodic solutions or chaotic motions in (2.1).

3. Second-order Subharmonic Resonance and Bifurcation

In this section we consider the second-order subharmonic resonance $\omega \approx 2a_1$ and set $\epsilon\Omega = (\omega^2 - 4a_1^2)/4$. Replace p and f by ϵp and ϵf ($0 < \epsilon \ll 1$), respectively, and

then (1.1) can be written as

$$\begin{cases} \dot{x} = y, \\ \dot{y} = -\omega_0^2 x - \beta x^3 - \gamma x^5 - \epsilon p(x^2 - 1)y + \epsilon f \cos \omega t. \end{cases} \quad (3.1)$$

Using regular perturbation methods, one obtains harmonic of (1.1) as

$$\bar{x}(t) = x_0 - \epsilon(f/(\omega^2 - a_1^2)) \cos \omega t + O(\epsilon^2). \quad (3.2)$$

To investigate stability of the harmonic $\bar{x}(t)$, one can set

$$x = \bar{x}(t) + \sqrt{\epsilon}z = x_0 + \sqrt{\epsilon}z - \epsilon\Gamma \cos \omega t + O(\epsilon^2), \quad (3.3)$$

where $\Gamma = f/(3a_1^2)(= f/(\omega^2 - a_1^2) + O(\epsilon^2))$, and $(x_0, 0)$ is a center of (3.1) for $\epsilon = 0$. Substituting (3.3) into (3.1), then (3.1) becomes

$$\ddot{z} + a_1^2 z = -\sqrt{\epsilon}a_2 z^2 + \epsilon(a_3 z^3 + 2a_2 z \Gamma \cos \omega t - p\alpha \dot{z}) + O(\epsilon^{3/2}). \quad (3.4)$$

Note that $\omega = 2a_1 + O(\epsilon^2)$.

Using the Van der Pol transformation

$$\begin{pmatrix} u \\ v \end{pmatrix} = \begin{pmatrix} \cos \frac{\omega t}{2} & -\frac{2}{\omega} \sin \frac{\omega t}{2} \\ -\sin \frac{\omega t}{2} & -\frac{2}{\omega} \cos \frac{\omega t}{2} \end{pmatrix} \begin{pmatrix} z \\ \dot{z} \end{pmatrix}, \quad (3.5)$$

in (3.1) and carrying out averaging up to second order, one has

$$\begin{aligned} \dot{u} &= \frac{\epsilon}{2a_1} ((\Omega - a_2\Gamma)v - p\alpha a_1 u + b_0 v(u^2 + v^2)), \\ \dot{v} &= \frac{\epsilon}{2a_1} ((-\Omega - a_2\Gamma)u - p\alpha a_1 v - b_0 u(u^2 + v^2)). \end{aligned} \quad (3.6)$$

In polar coordinates, (3.6) becomes

$$\begin{aligned} \dot{r} &= \frac{\epsilon}{2a_1} (-p\alpha a_1 - a_2\Gamma \sin 2\theta)r, \\ r\dot{\theta} &= \frac{\epsilon}{2a_1} (-\Omega - b_0 r^3 - a_2\Gamma \cos 2\theta). \end{aligned} \quad (3.7)$$

By analyzing the fixed points of (3.7), we have the following conclusion.

Lemma 3.1. (i) (3.6) always has a trivial equilibrium $(u, v) = (0, 0)$, which corresponds to the non-resonance harmonic $\bar{x}(t)$ of (3.2).

(ii) Assume that $a_2^2\Gamma^2 - p^2\alpha^2 a_1^2 > 0$, and $b_0(-\Omega \pm \sqrt{a_2^2\Gamma^2 - p^2\alpha^2 a_1^2}) > 0$, then (3.7) has fixed points with $r > 0$ at $(r, \theta) = (r_{\pm}, \theta_{\pm})$, and $(r, \theta) = (r_{\pm}, \theta_{\pm} + \pi)$ where $r_{\pm} = \frac{-\Omega \pm \sqrt{a_2^2\Gamma^2 - p^2\alpha^2 a_1^2}}{b_0}$, and if $a_2\alpha > 0$, then

$$\theta_+ = -\frac{1}{2} \arcsin \frac{p\alpha a_1}{a_2\Gamma}, \quad \theta_- = \frac{\pi}{2} - \theta_+, \quad (3.8)$$

and if $a_2\alpha < 0$, then

$$\theta_- = -\frac{1}{2} \arcsin \frac{p\alpha a_1}{a_2\Gamma}, \quad \theta_+ = \frac{\pi}{2} - \theta_-. \quad (3.9)$$

Lemma 3.2. (i) (3.6) always has a trivial fixed point $(0, 0)$, which is a saddle point for $a_2^2 \Gamma^2 > \Omega^2 + p^2 \alpha^2 a_1^2$, and which is a stable or an unstable for $a_2^2 \Gamma^2 < \Omega^2 + p^2 \alpha^2 a_1^2$ and $\alpha > 0$ or $\alpha < 0$.

(ii) If $b_0 > 0$, then the fixed points (r_+, θ_+) and $(r_+, \theta_+ + \pi)$ are stable foci-node for $\alpha > 0$ or unstable foci-node for $\alpha < 0$ and the others are saddles. If $b_0 < 0$, then the fixed points (r_+, θ_+) and $(r_+, \theta_+ + \pi)$ are saddles and the others are stable foci-node for $\alpha > 0$ or unstable for $\alpha < 0$.

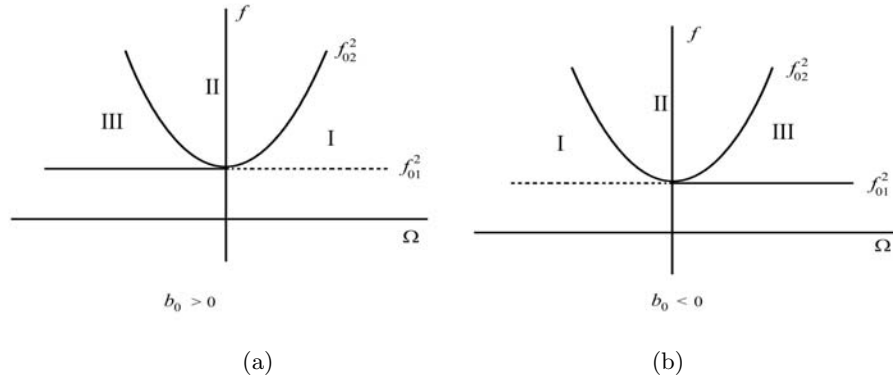


Figure 3. Super-critical and sub-critical saddle-node bifurcation curves: (a) $b_0 > 0$; (b) $b_0 < 0$.

By the averaging theorem we get the following conclusion.

Theorem 3.1. (i) Including the trivial fixed point $(0, 0)$, there is one, three, or five fixed points in (3.7). Each pair of nontrivial fixed point (r_{\pm}, θ_{\pm}) and $(r_{\pm}, \theta_{\pm} + \pi)$ corresponds to a single second-order subharmonic of (3.1), which is approximately given by

$$x = x_0 + \sqrt{\epsilon} \cos\left(\frac{1}{2}\omega t + \theta_{\pm}\right) - \epsilon \Gamma \cos \omega t. \quad (3.10)$$

(ii) There are two bifurcation curves: saddle-node bifurcations of subharmonics occur near the curve

$$f^2 = \frac{9p^2 \alpha^2 a_1^6}{a_2^2} \equiv f_{01}^2, \quad b_0 \Omega < 0 \quad (3.11)$$

and period doubling bifurcations of harmonics occur near the curve

$$f^2 = \frac{9a_1^4 (\Omega^2 + p^2 \alpha^2 a_1^2)}{a_2^2} \equiv f_{02}^2, \quad (3.12)$$

which is supercritical if $b_0 \Omega > 0$ and subcritical if $b_0 \Omega < 0$.

(iii) In region (I), there is a stable fixed points $(0, 0)$ of (3.6), which corresponds to a stable (resp. unstable) non-resonant harmonic of (3.1) for $\alpha > 0$ and an unstable fixed points $(0, 0)$ of (3.6), which corresponds to an unstable non-resonant harmonic of (3.1) for $\alpha < 0$; in region (II), there are three fixed points and one of them corresponds to a unstable non-resonant harmonic and

a single stable resonant subharmonic of period-two of (3.1) for $\alpha > 0$ and a single unstable resonant subharmonic of period-two of (3.1) for $\alpha < 0$; in region (III), there are five fixed points which correspond to a stable non-resonant harmonic and a stable resonant subharmonic for $\alpha > 0$ or an unstable non-resonant harmonic and an unstable resonant subharmonic for $\alpha < 0$ and an unstable resonant subharmonic of (3.1), where the regions(I)-(III) are in Fig.3.

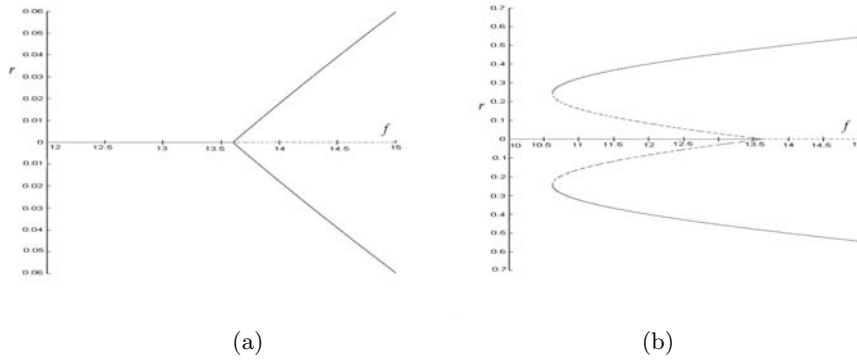


Figure 4. Bifurcation diagrams of fixed points of (3.7). (a) Passing through regions I and II in Fig.3(a) for $\Omega = 6$; (b) passing through regions I, III and II in Fig.3(a) for $\Omega = -6$. Stable orbits are shown solid, and unstable orbits dashed.

Fig.4 shows a bifurcation diagram indicating how the fixed points of (3.7) are created or annihilated, passing through the regions (I)-(III), when f is varying while the other parameters are fixed as $\beta = -2, \gamma = 0.5, \omega = 1, p = 1, \alpha = 2.41442, a_1 = 3.10755, b_0 = 24.8088$.

4. Third-order Subharmonic Resonance and Bifurcation

We consider the third-order subharmonic resonance $\omega = 3a_1$ and set $\epsilon^2\Omega = (\omega^2 - 9a_1^2)/9$. Replace p and f by ϵ^2p and ϵf ($0 < \epsilon \ll 1$), respectively, and then (1.1) can be written as

$$\begin{cases} \dot{x} = y, \\ \dot{y} = -\omega_0^2x - \beta x^3 - \gamma x^5 - \epsilon^2p(x^2 - 1)y + \epsilon f \cos \omega t. \end{cases} \quad (4.1)$$

Using perturbation methods, one obtains a periodic solution of period $2\pi/\omega$ to equation (4.1),

$$\bar{x}(t) = x_0 + \epsilon x_1(t) + \epsilon^2 x_2(t) + O(\epsilon^3), \quad (4.2)$$

where

$$\begin{aligned} x_1(t) &= \frac{f}{a_1^2 - \omega^2} \cos \omega t, \\ x_2(t) &= -\frac{a_2 f^2}{2a_1^2(a_1^2 - \omega^2)^2} - \frac{a_2 f^2}{2(a_1^2 - 4\omega^2)(a_1^2 - \omega^2)^2} \cos 2\omega t. \end{aligned} \quad (4.3)$$

Let

$$x = \bar{x}(t) + \epsilon z = x_0 + \epsilon(z - \Gamma \cos \omega t) + \epsilon^2 \left(\frac{a_2 \Gamma^2}{70 a_1^2} \right) (35 - \cos 2\omega t) + O(\epsilon^3), \quad (4.4)$$

where $\Gamma = \frac{f}{8a_1^2} (= \frac{f}{\omega^2 - a_1^2} + O(\epsilon^2))$, and $(x_0, 0)$ is a center of (4.1) for $\epsilon = 0$.

Substituting (4.4) into (4.1), then (4.1) becomes

$$\begin{aligned} \ddot{z} + a_1^2 z &= -\epsilon a_2 (z - 2\Gamma \cos \omega t) z + \epsilon^2 (a_3 (z - \Gamma \cos \omega t)^3 \\ &\quad - \frac{a_2^2 \Gamma^2}{35 a_1^2} (z - \Gamma \cos \omega t) (35 - \cos 2\omega t) - p\alpha (\dot{z} + \omega \Gamma \sin \omega t)) + O(\epsilon^3). \end{aligned} \quad (4.5)$$

Note that $\omega = 3a_1 + O(\epsilon^2)$.

Using the Van der Pol transformation

$$\begin{pmatrix} u \\ v \end{pmatrix} = \begin{pmatrix} \cos \frac{\omega t}{3} & -\frac{3}{\omega} \sin \frac{\omega t}{3} \\ -\sin \frac{\omega t}{3} & -\frac{3}{\omega} \cos \frac{\omega t}{3} \end{pmatrix} \begin{pmatrix} z \\ \dot{z} \end{pmatrix}, \quad (4.6)$$

in (4.5) and averaging up to second order, one has

$$\begin{aligned} \dot{u} &= \frac{\epsilon^2}{2a_1} (-p\alpha a_1 u + (\Omega + b_1 \Gamma^2)v + b_0 v(u^2 + v^2) + 2b_2 \Gamma uv), \\ \dot{v} &= \frac{\epsilon^2}{2a_1} (-p\alpha a_1 v - (\Omega + b_1 \Gamma^2)u - b_0 u(u^2 + v^2) + b_2 \Gamma(u^2 - v^2)), \end{aligned} \quad (4.7)$$

where $b_0 = \frac{10a_2^2 + 9a_1^2 a_3}{12a_1^2}$, $b_1 = \frac{15a_3 a_1^2 - 14a_2^2}{10a_1^2}$ and $b_2 = \frac{3a_3 a_1^2 - 2a_2^2}{4a_1^2}$.

In polar coordinates, (4.7) becomes

$$\begin{aligned} \dot{r} &= \frac{\epsilon^2}{2a_1} (-p\alpha a_1 r - b_2 \Gamma r^2 \sin 3\theta), \\ \dot{\theta} &= \frac{\epsilon^2}{2a_1} (-(\Omega + b_1 \Gamma^2) - b_0 r^2 + b_2 \Gamma r \cos 3\theta). \end{aligned} \quad (4.8)$$

(4.7) has the trivial fixed point $(u, v) = (0, 0)$, which corresponds to a non-resonant harmonic $\bar{x}(t)$ of (4.1). The trivial fixed point is stable for $\alpha > 0$ and unstable for $\alpha < 0$. The nontrivial fixed points satisfy the following equation

$$b_0^2 r^4 + (2b_0(\Omega + b_1 \Gamma^2) - b_2^2 \Gamma^2) r^2 + (\Omega + b_1 \Gamma^2)^2 + p^2 \alpha^2 a_1^2 = 0. \quad (4.9)$$

If

$$b_2^2 \Gamma^2 - 2b_0(\Omega + b_1 \Gamma^2) > 2|b_0| \sqrt{(\Omega + b_1 \Gamma^2)^2 + p^2 \alpha^2 a_1^2}, \quad (4.10)$$

then (4.8) has nontrivial fixed points at $(r, \theta) = (r_{\pm}, \theta_{\pm} + 2j\pi/3), (j = 0, 1, 2)$, where

$$r_{\pm} = \frac{\sqrt{2}}{2|b_0|} \sqrt{b_2^2 \Gamma^2 - 2b_0(\Omega + b_1 \Gamma^2) \pm \sqrt{(b_2^2 - 4b_0 b_1) b_2^2 \Gamma^4 - 4b_0 b_2^2 \Omega \Gamma^2 - 4b_0^2 p^2 \alpha^2 a_1^2}} \quad (4.11)$$

and

$$\theta_{\pm} = \frac{1}{3} \arcsin \frac{p\alpha a_1}{b_2 \Gamma r_{\pm}} \quad \text{or} \quad \theta_{\pm} = \frac{\pi}{3} - \frac{1}{3} \arcsin \frac{p\alpha a_1}{b_2 \Gamma r_{\pm}}. \quad (4.12)$$

By further detailed analysis for fixed points of (4.8), we can get the following conclusion.

Lemma 4.1. (i) If $b_2^2 > 4b_0b_1$ and $f^2 > f_1^2$, then there exist six nontrivial fixed points and one trivial fixed point $(0, 0)$, where

$$f_1^2 = \frac{128a_1^4(2b_0|b_2|\Omega + 2|b_0|\sqrt{b_2^2\Omega^2 + (b_2^2 - 4b_0b_1)p^2\alpha^2a_1^2})}{|b_2|(b_2^2 - 4b_0b_1)}. \quad (4.13)$$

(ii) If $b_2^2 = 4b_0b_1$ and $f^2 > f_2^2$, then there exist six nontrivial fixed points and one trivial fixed point $(0, 0)$, where

$$f_2^2 = \frac{-b_2^2p^2\alpha^2a_1^2}{b_0b_2^2\Omega}, \quad b_0\Omega < 0. \quad (4.14)$$

(iii) If $b_2^2 < 4b_0b_1$, $b_0\Omega < 0$ and $f_1^2 < f^2 < f_3^2$, then there exist six nontrivial fixed points and one trivial fixed point $(0, 0)$, where

$$f_3^2 = \frac{128a_1^4(2b_0|b_2|\Omega - 2|b_0|\sqrt{b_2^2\Omega^2 + (b_2^2 - 4b_0b_1)p^2\alpha^2a_1^2})}{|b_2|(b_2^2 - 4b_0b_1)}. \quad (4.15)$$

The fixed points $(r_+, \theta_+ + 2j\pi/3)$, $j = 0, 1, 2$, are stable (resp. unstable) foci-node for $\alpha > 0$ (resp. $\alpha < 0$), and $(r_-, \theta_- + 2j\pi/3)$, $j = 0, 1, 2$ are saddles. Each triple of fixed points $(r_\pm, \theta_\pm + 2j\pi/3)$, $j = 0, 1, 2$ corresponds to a single third-order subharmonic of (4.1), which is approximately given by

$$x = x_0 + \epsilon r_\pm \cos\left(\frac{\omega t}{3} + \theta_\pm\right) - \epsilon \Gamma \cos \omega t + O(\epsilon^2). \quad (4.16)$$

From the averaging theorem, we have the following theorem.

Theorem 4.1. (i) If $b_2^2 > 4b_0b_1$ and $f^2 > f_1^2$, there exist two resonant third-order subharmonics and a nonresonant harmonic, and supercritical saddle-node bifurcations of third-order subharmonics occur near the curve (4.13).

(ii) If $b_2^2 = 4b_0b_1$ and $f^2 > f_2^2$, there exist two resonant third-order subharmonics and a nonresonant harmonic, and supercritical saddle-node bifurcations of third-order subharmonics occur near the curve (4.14).

(iii) If $b_2^2 < 4b_0b_1$ and $f_1^2 < f^2 < f_3^2$, there exist two resonant third-order subharmonics and a nonresonant harmonic, and supercritical saddle-node bifurcations of subharmonics occur near the curve (4.13) and subcritical saddle-node bifurcations occur near the curve (4.15).

5. The m-Order Subharmonics and Bifurcation

In this section we investigate the existence of m -order subharmonics of (1.1) by using Melnikov's method for subharmonic which is defined in [23].

Consider the perturbed system

$$\begin{cases} \dot{x} = y, \\ \dot{y} = -\omega_0^2 x - \beta x^3 - \gamma x^5 - \epsilon p(x^2 - 1)y + \epsilon f \cos \omega t. \end{cases} \quad (5.1)$$

Let $q^\mu(t) = (x^\mu(t), y^\mu(t))$ ($\mu \in (\mu_1, \mu_2)$) denote a one-parameter family of periodic orbits with period $\frac{2\pi m}{n\omega}$ of (5.1) for $\epsilon = 0$, where μ_1 and μ_2 are constants, and

m and n are relatively prime. In [24], it has been proved that $M^m(t_0)$ can have simple zero only if $n = 1$, so the Melnikov function for $q^\mu(t)$ of (5.1) is given by

$$\begin{aligned} M^m(t_0) &= \int_0^{\frac{2\pi m}{\omega}} y^\mu(t) [-p((x^\mu(t))^2 - 1)y^\mu(t) + f \cos \omega(t + t_0)] dt \\ &= -pA^m(\omega_0, \beta, \gamma) + fD^m(\omega_0, \beta, \gamma, \omega) \cos \omega t_0 + \Theta^m(\omega_0, \beta, \gamma, \omega), \end{aligned} \quad (5.2)$$

where

$$\begin{aligned} A^m(\omega_0, \beta, \gamma) &= \int_0^{\frac{2\pi m}{\omega}} ((x^\mu(t))^2 - 1)(y^\mu(t))^2 dt, \\ B^m(\omega_0, \beta, \gamma, \omega) &= \int_0^{\frac{2\pi m}{\omega}} y^\mu(t) \cos \omega t dt, \\ C^m(\omega_0, \beta, \gamma, \omega) &= \int_0^{\frac{2\pi m}{\omega}} y^\mu(t) \sin \omega t dt, \\ D^m(\omega_0, \beta, \gamma, \omega) &= \sqrt{(B^m(\omega_0, \beta, \gamma, \omega))^2 + (C^m(\omega_0, \beta, \gamma, \omega))^2}, \\ \Theta^m(\omega_0, \beta, \gamma, \omega) &= \arctan \frac{C^m}{B^m}. \end{aligned} \quad (5.3)$$

If

$$\frac{f}{p} > \left| \frac{A^m}{B^m} \right| \equiv R^m(\omega_0, \beta, \gamma, \omega), \quad (5.4)$$

then $M^m(t_0)$ has a simple zero and a necessary condition for the occurrence of subharmonics of period $\frac{2\pi m}{\omega}$ of (5.1) is given by (5.4).

The bifurcation curve of subharmonic is created and occurs at

$$\frac{f}{p} = \left| \frac{A^m}{B^m} \right| = R^m(\omega_0, \beta, \gamma, \omega) + O(\epsilon). \quad (5.5)$$

6. Superharmonic Resonance and Bifurcation

In this section we consider superharmonic resonance using the second-order averaging method. For the case of third-order superharmonic resonance $3\omega \approx a_1$, one sets $\epsilon^2 \Omega = 9\omega^2 - a_1^2$. Replace p and f by $\epsilon^2 p$ and ϵf ($0 < \epsilon \ll 1$), respectively, and then (1.1) can be written as

$$\begin{cases} \dot{x} = y, \\ \dot{y} = -\omega_0^2 x - \beta x^3 - \gamma x^5 - \epsilon^2 p(x^2 - 1)y + \epsilon f \cos \omega t. \end{cases} \quad (6.1)$$

Let

$$x = x_0 + \epsilon \Gamma \cos \omega t + \epsilon z, \quad (6.2)$$

where $\Gamma = \frac{9f}{8a_1^2} (= \frac{f}{a_1^2 - \omega^2} + O(\epsilon))$, and $(x_0, 0)$ is a center of (6.1) for $\epsilon = 0$.

Substituting (6.2) into (6.1), then (6.1) becomes

$$\ddot{z} + a_1^2 z = -\epsilon a_2 (z + \Gamma \cos \omega t)^2 + \epsilon^2 \{a_3 (z + \Gamma \cos \omega t)^3 - p\alpha (\dot{z} - \Gamma \omega \sin \omega t)\} + O(\epsilon^3). \quad (6.3)$$

Using the Van der Pol transformation

$$\begin{pmatrix} u \\ v \end{pmatrix} = \begin{pmatrix} \cos 3\omega t & -\frac{1}{3\omega} \sin 3\omega t \\ -\sin 3\omega t & -\frac{1}{3\omega} \cos 3\omega t \end{pmatrix} \begin{pmatrix} z \\ \dot{z} \end{pmatrix}, \quad (6.4)$$

in (6.3) and averaging up to second order, one has

$$\begin{aligned} \dot{u} &= \frac{\epsilon^2}{2a_1}(-p\alpha a_1 u + (\Omega + b_3\Gamma^2)v + b_0v(u^2 + v^2)), \\ \dot{v} &= \frac{\epsilon^2}{2a_1}(-p\alpha a_1 v - (\Omega + b_3\Gamma^2)u - b_0u(u^2 + v^2) - b_4\Gamma^3), \end{aligned} \quad (6.5)$$

where $b_0 = \frac{10a_2^2 + 9a_3a_1^2}{12a_1^2}$, $b_3 = \frac{106a_2^2 + 105a_1^2a_3}{70a_1^2}$ and $b_4 = \frac{18a_2^2 + 5a_3a_1^2}{20a_1^2}$.

In polar coordinates, (6.5) becomes

$$\begin{aligned} \dot{r} &= \frac{\epsilon^2}{2a_1}(-p\alpha a_1 r - b_4\Gamma^3 \sin \theta), \\ r\dot{\theta} &= \frac{\epsilon^2}{2a_1}(-(\Omega + b_3\Gamma^2)r - b_0r^3 - b_4\Gamma^3 \cos \theta). \end{aligned} \quad (6.6)$$

Fixed points of (6.6) satisfy the following equation

$$b_0^2 r^6 + 2b_0(\Omega + b_3\Gamma^2)r^4 + ((\Omega + b_3\Gamma^2)^2 + p^2\alpha^2 a_1^2)r^2 - b_4^2\Gamma^6 = 0, \quad (6.7)$$

and $\theta = \arctan \frac{p\alpha a_1}{(\Omega + b_3\Gamma^3) + b_0r^2}$.

Note that

$$F_1 = \frac{1}{27b_0}(-2((b_3\Gamma^2 + \Omega)^3 + 9p^2\alpha^2 a_1^2(b_3\Gamma^2 + \Omega)) - 2((b_3\Gamma^2 + \Omega)^2 - 3p^2\alpha^2 a_1^2)^{\frac{3}{2}}), \quad (6.8)$$

and

$$F_2 = \frac{1}{27b_0}(-2((b_3\Gamma^2 + \Omega)^3 + 9p^2\alpha^2 a_1^2(b_3\Gamma^2 + \Omega)) + 2((b_3\Gamma^2 + \Omega)^2 - 3p^2\alpha^2 a_1^2)^{\frac{3}{2}}). \quad (6.9)$$

By the analysis for fixed points and stability of (6.6), we obtain the following conclusion.

Lemma 6.1. (i) If $b_0(\Omega + b_3\Gamma^2) > 0$, then (6.6) has a nontrivial fixed point, which is stable for $\alpha > 0$ and unstable for $\alpha < 0$.

(ii) If $b_0(\Omega + b_3\Gamma^2) < 0$ and $(\Omega + b_3\Gamma^2)^2 \leq 3p^2\alpha^2 a_1^2$, (6.6) has a nontrivial fixed point, which is stable for $\alpha > 0$ and unstable for $\alpha < 0$. And if $(\Omega + b_3\Gamma^2)^2 = 3p^2\alpha^2 a_1^2$ and $b_4^2\Gamma^6 = -\frac{8}{27b_0}(\Omega + b_3\Gamma^2)^3$, (6.6) has three coincide nontrivial fixed points with one zero eigenvalue.

(iii) If $b_0 > 0$, $\Omega + b_3\Gamma^2 < 0$, and $(\Omega + b_3\Gamma^2)^2 > 3p^2\alpha^2 a_1^2$, when $b_4^2\Gamma^6 > F_2$ or $b_4^2\Gamma^6 < F_1$, (6.6) has a nontrivial fixed point, which is stable for $\alpha > 0$ and unstable for $\alpha < 0$; when $b_4^2\Gamma^6 = F_2$ or $b_4^2\Gamma^6 = F_1$, (6.6) has two distinct nontrivial fixed points, one of which has one zero eigenvalue; when $F_1 < b_4^2\Gamma^6 < F_2$, (6.6) has three distinct nontrivial fixed points and one of them is a saddle point and others are stable for $\alpha > 0$ and unstable for $\alpha < 0$.

(iv) If $b_0 < 0$, $\Omega + b_3\Gamma^2 > 0$, and $(\Omega + b_3\Gamma^2)^2 > 3p^2\alpha^2 a_1^2$, when $b_4^2\Gamma^6 > F_1$ or $b_4^2\Gamma^6 < F_2$, (6.6) has a nontrivial fixed point, which is stable for $\alpha > 0$ and unstable for $\alpha < 0$; when $b_4^2\Gamma^6 = F_1$ or $b_4^2\Gamma^6 = F_2$, (6.6) has two distinct nontrivial fixed points, one of which has one zero eigenvalue; when $F_2 < b_4^2\Gamma^6 < F_1$, (6.6) has three distinct nontrivial fixed points and one of them is a saddle point and others are stable for $\alpha > 0$ and unstable for $\alpha < 0$.

Each nontrivial fixed point (r, θ) corresponds to a third-order superharmonic of (6.1), which is approximately given by

$$x = x_0 + \epsilon \Gamma \cos \omega t + \epsilon r \cos(3\omega t + \theta) + O(\epsilon^2). \quad (6.10)$$

From the averaging theorem, we have the following theorem.

Theorem 6.1. (i) *If $b_0(\Omega + b_3\Gamma^2) > 0$, there exists one resonant third-order superharmonic.*

(ii) *If $b_0(\Omega + b_3\Gamma^2) < 0$ and $(\Omega + b_3\Gamma^2)^2 \leq 3p^2\alpha^2a_1^2$, there exists one resonant third-order superharmonic.*

(iii) *If $b_0 > 0$, $\Omega + b_3\Gamma^2 < 0$ and $(\Omega + b_3\Gamma^2)^2 > 3p^2\alpha^2a_1^2$, then there exists one resonant third-order superharmonic for $b_4^2\Gamma^6 > F_2$ or $b_4^2\Gamma^6 < F_1$, and there exist three resonant third-order superharmonics for $F_2 < b_4^2\Gamma^6 < F_1$. Supercritical saddle-node bifurcation of third-order superharmonic occurs near the curve $b_4^2\Gamma^6 = F_2$ and subcritical saddle-node bifurcation of third-order superharmonic occurs near the curve $b_4^2\Gamma^6 = F_1$.*

(iv) *If $b_0 < 0$, $\Omega + b_3\Gamma^2 > 0$ and $(\Omega + b_3\Gamma^2)^2 > 3p^2\alpha^2a_1^2$, then there exists one resonant third-order superharmonic for $b_4^2\Gamma^6 > F_1$ or $b_4^2\Gamma^6 < F_2$, and there exist three resonant third-order superharmonics for $F_1 < b_4^2\Gamma^6 < F_2$. Supercritical saddle-node bifurcation of third-order superharmonic occurs near the curve $b_4^2\Gamma^6 = F_1$ and subcritical saddle-node bifurcation of third-order superharmonic occurs near the curve $b_4^2\Gamma^6 = F_2$.*

7. Chaos in Equation (1.1)

In this section, we discuss the chaotic behaviors of equation (1.1) in which f and p are assumed to be small parameters with order ϵ . Rewriting (1.1) as an autonomous system gives

$$\begin{cases} \dot{x} = y, \\ \dot{y} = -\omega_0^2 x - \beta x^3 - \gamma x^5 + \epsilon(\bar{f} \cos \phi - p_1(x^2 - 1)y), \\ \dot{\phi} = \omega, \end{cases} \quad (7.1)$$

where $\epsilon\bar{f} = f, \epsilon p_1 = p$.

The unperturbed system of system (7.1) has two homoclinic orbits Γ_{hom}^\pm and two heteroclinic orbits Γ_{het}^\pm for $\gamma > 0, \beta < 0$ and $\beta^2 - 4\gamma\omega_0^2 > 0$. The phase portrait of the unperturbed system is shown in Fig.5(a) for $\omega_0 = 1, \beta = -3$, and $\gamma = 2$. When the perturbation is added, the homoclinic or heteroclinic orbits break, and may have transverse homoclinic or heteroclinic orbits. By the Smale-Birkhoff homoclinic theorem [3, 23], the existence of such orbits results in chaotic dynamics. We therefore apply the Melnikov method to equation (7.1) for finding the criteria of the existence of homoclinic or heteroclinic bifurcation and chaos.

Suppose that the homoclinic or heteroclinic orbits of the unperturbed systems are written as $(x_0(t), y_0(t))$, then the Melnikov function for system (7.1) can be given

$$M(t_0) = -p_1 \int_{-\infty}^{+\infty} (x_0^2(t) - 1)y_0^2(t)dt + \int_{-\infty}^{+\infty} y_0(t)\bar{f} \cos(\omega(t + t_0))dt, \quad (7.2)$$

where t_0 is the cross-section time of the Poincaré map and t_0 can be interpreted as the initial time of the forcing term.

Because it is difficult to give analytical expression of $(x_0(t), y_0(t))$, we will compute $x_0(t)$ and $y_0(t)$ numerically. We note that $y_0(t)$ is a function of time from $-\infty$ to $+\infty$. We therefore choose a starting point P_1 which is an intersecting point of homoclinic orbit Γ_{hom}^\pm with x -axis, and a starting point P_2 which is an intersecting point of heteroclinic orbit Γ_{het}^\pm with y -axis, and $y_0(t)$ would be an odd function of time for the homoclinic orbit and an even function of time for the heteroclinic orbit (see Fig.5(a)).

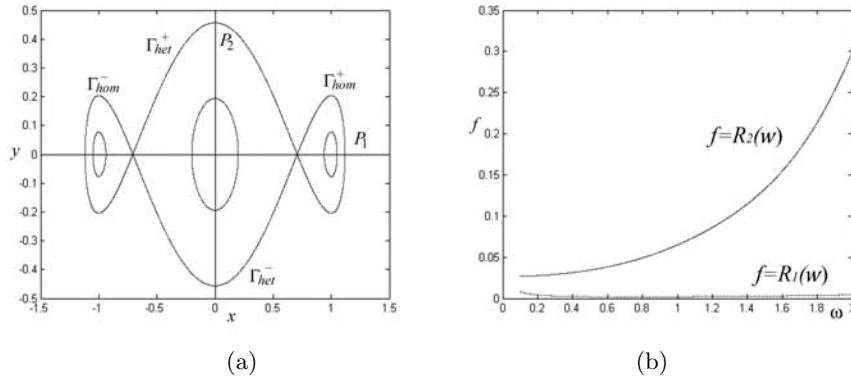


Figure 5. (a) The phase portrait of unperturbed system of (7.1). (b) The homoclinic bifurcation curve (7.5) and heteroclinic bifurcation curve (7.8). Here $\beta = -3, \gamma = 2, \omega_0 = 1, p = 0.1$.

For the homoclinic orbits Γ_{hom}^\pm , the Melnikov function can be simplified as

$$\begin{aligned} M_1(t_0) &= -2p_1 \int_0^{+\infty} (x_0^2(t) - 1)y_0^2(t)dt - 2\bar{f} \sin(\omega t_0) \int_0^{+\infty} y_0(t) \sin(\omega t)dt \\ &= -2p_1 A - 2\bar{f} \sin(\omega t_0) I_{hom1}(\omega), \end{aligned} \quad (7.3)$$

where $A = \int_0^{+\infty} (x_0^2(t) - 1)y_0^2(t)dt$ is a constant once $x_0(t)$ and $y_0(t)$ are given, $I_{hom1}(\omega) = \int_0^{+\infty} y_0(t) \sin(\omega t)dt$ is a function of the frequency ω when the homoclinic orbits $(x_0(t), y_0(t))$ are given. Thus, if

$$\bar{f} > \left| \frac{p_1 A}{I_{hom1}(\omega)} \right| \quad \text{or} \quad f > \left| \frac{pA}{I_{hom1}(\omega)} \right| \equiv R_1(\omega), \quad (7.4)$$

then there is a \bar{t}_0 such that $M_1(\bar{t}_0) = 0$ and $\frac{\partial M_1}{\partial t_0}|_{t=\bar{t}_0} \neq 0, \bar{t}_0 \in [0, \frac{2\pi}{\omega}]$ and the following theorem can be obtained.

Theorem 7.1. *The homoclinic bifurcation will occur at*

$$f = R_1(\omega), \quad (7.5)$$

this implies that if $\varepsilon > 0$ is sufficiently small, the transverse homoclinic orbits exist and system (7.1) may be chaotic.

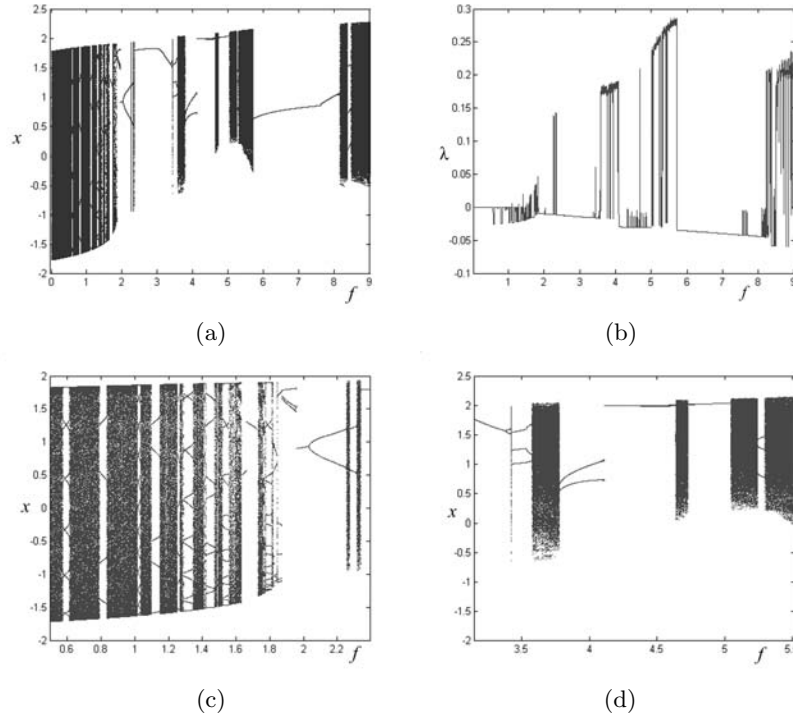


Figure 6. (a) Bifurcation diagram of system (1.1) in (f, x) plane for $\beta = -3, \gamma = 2, p = 0.1, \omega_0 = 1, \omega = 1$; (b) maximal Lyapunov exponent corresponding to (a); (c) local amplification of (a) for $0.6 < f < 2.2$; (d) local amplification of (a) for $3.5 < f < 5.5$.

For the heteroclinic orbits, $y_0(t)$ is even, then the Melnikov function on Γ_{het}^\pm can be written as

$$\begin{aligned} M_2(t_0) &= -2p_1 \int_0^{+\infty} (x_0^2(t) - 1)y_0^2(t)dt - 2\bar{f} \cos(\omega t_0) \int_0^{+\infty} y_0(t) \cos(\omega t)dt \\ &= -2p_1 B - 2\bar{f} \cos(\omega t_0) I_{het}(\omega), \end{aligned} \quad (7.6)$$

where $B = \int_0^{+\infty} (x_0^2(t) - 1)y_0^2(t)dt$, $I_{het}(\omega) = \int_0^{+\infty} y_0(t) \cos(\omega t)dt$ is a function of the frequency ω when the heteroclinic orbits $(x_0(t), y_0(t))$ are given. Thus, if

$$\bar{f} > \left| \frac{p_1 B}{I_{het}(\omega)} \right| \quad \text{or} \quad f > \left| \frac{pB}{I_{het}(\omega)} \right| \equiv R_2(\omega), \quad (7.7)$$

then there is a \bar{t}_0 such that $M_2(\bar{t}_0) = 0$ and $\frac{\partial M_1}{\partial t_0}|_{t=\bar{t}_0} \neq 0, \bar{t}_0 \in [0, \frac{2\pi}{\omega}]$ and the following theorem can be obtained.

Theorem 7.2. *The heteroclinic bifurcation will occur at*

$$f = R_2(\omega), \quad (7.8)$$

this implies that if $\varepsilon > 0$ is sufficiently small, the transverse heteroclinic orbits exist and system (1.1) may be chaotic.

The homoclinic bifurcation (7.5) and heteroclinic bifurcation curve (7.8) are shown in Fig.5(b) for $\beta = -3, \gamma = 2, \omega_0 = 1, p = 0.1$.

8. Numerical Simulation

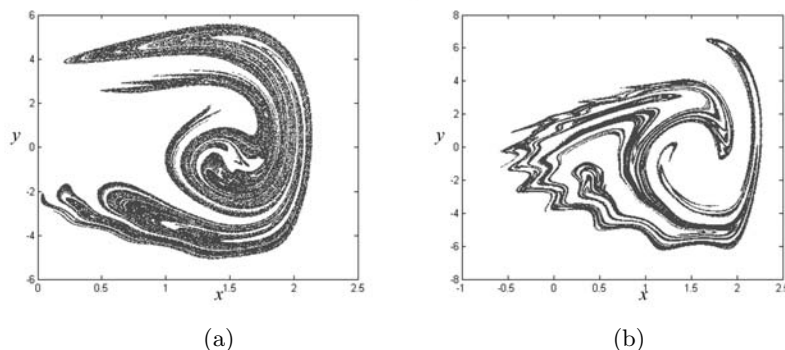


Figure 7. Chaotic attractors in Poincaré map of system (1.1): (a) for $f = 5.5$ in Fig.6(a); (b) for $f = 8.95$ in Fig.6(a).

Now we present some numerical simulation results to find other complex dynamical behaviors of system (1.1). The bifurcation parameters are considered in the following six cases.

- (1) Varying f in the range $0 \leq f \leq 9$ and fixing $p = 0.1, \beta = -3, \gamma = 2, \omega = 1$ (which are the same with previously case (1) in [7]) and for rational and irrational values of ω_0 .
- (2) Varying ω_0 in the range $0 \leq \omega_0 \leq 2$ and fixing $p = 1, \beta = -3, \gamma = 2, f = 2$ and $\omega = 1$, (which are the same with previously case (3) in [7])
- (3) Varying γ in the range $0.1 \leq \gamma \leq 3$ and fixing $p = 1, \beta = -3, \omega = 1, f = 2$ (which are the same with previously case (4) in [7]) and for rational and irrational values of ω_0 .
- (4) Varying β in the range $-6 \leq \beta \leq 2$ and fixing $p = 1, \gamma = 2, \omega = 1, f = 2$ (which are the same with previously case (5) in [7]) and for rational and irrational values of ω_0 .
- (5) Varying p in the range $0 \leq p \leq 7$ and fixing $\beta = -3, \gamma = 2, \omega = 1, f = 2$ (which are the same with previously case (6) in [7]) and for rational and irrational values of ω_0 .
- (6) Varying ω in the range $0 \leq \omega \leq 6$ and fixing $p = 0.1, \beta = -3, \gamma = 2$ (which are the same with previously case (7) in [7]) for several values of f and rational and irrational values of ω_0 .

Remark. In order to compare the dynamical behavior of system (1.1) with that in [7], we take up with the same values for each case. And we show the differences of bifurcation diagrams and dynamical behaviors of system (1.1) and the system in [7] from the following results.

For case (1). The bifurcation diagram of system (1.1) in (f, x) plane and the corresponding maximum Lyapunov exponents for $\omega_0 = 1$ are given in Fig.6(a) and (b), and the local amplified bifurcation diagrams of Fig.6(a) for $f \in (0.6, 2.2)$, $f \in (3.5, 5.5)$ are shown in Fig.6(c) and (d), respectively. We observe chaotic regions with complex period windows including period 10, 4, 21, 5, 13, 9, 2, 13, 15, 3 orbits as f increasing, and with a more wide period one window. The chaotic attractors in Poincaré map of system (1.1) are shown in Fig.7(a) and (b) for $f = 5.5$, and $f = 8.95$, respectively.

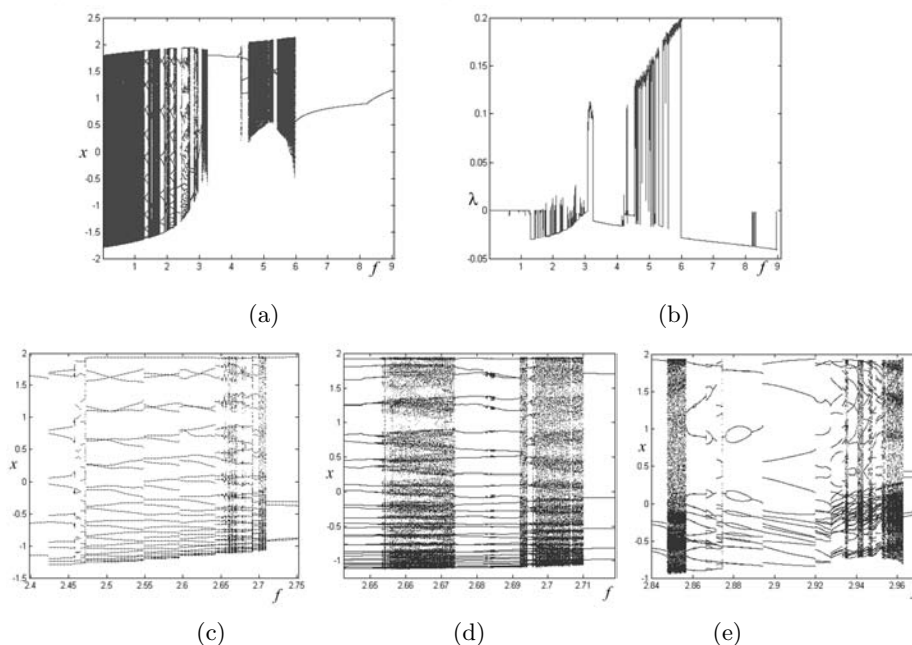


Figure 8. (a) Bifurcation diagram of system (1.1) in (f, x) plane for $\beta = -3, \gamma = 2, p = 0.1, \omega_0 = \sqrt{2}, \omega = 1$; (b) maximal Lyapunov exponent corresponding to (a); (c) local amplification of (a) for $2.4 < f < 2.75$; (d) local amplification of (a) for $2.65 < f < 2.71$ (e) local amplification of (a) for $2.84 < f < 2.97$.

The bifurcation diagram of system (1.1) in (f, x) plane and the corresponding maximum Lyapunov exponents for $\omega_0 = \sqrt{2}$, are shown in Fig.8(a) and (b), respectively. The local amplification of Fig.8(a) for $f \in (2.4, 2.75)$ and $f \in (2.64, 2.72)$ and $f \in (2.84, 2.97)$ are given in Fig.8(c), (d) and (e), respectively. We show that the onset of chaos and chaos suddenly disappearing to periodic one orbit at $f \approx 6$ in Fig.8(a), and the chaotic regions with the period-windows (periods-3, 5, 13, 17, 25, 27, 29, 31, 37, 41 orbits, and so on) and quasi-periodic orbits in Fig.8(c)-8(e). In Fig.8(e), there are the symmetry-breakings of 13 pairs and 9 pairs. The quasi-periodic orbits at $f = 2.05$ (maximum Lyapunov exponent $L = 0$) is given in Fig.9(a)(i) and (b)(i). The chaotic attractors at $f = 2.7$ ($L = 0.028958$) and at $f = 3.1$ ($L = 0.093943$) are given in Fig.9(a)(ii), (b)(ii) and Fig.9(a)(iii), (b)(iii), respectively, and the local amplification of (b)(ii) is shown in Fig.9(b)(ii)*. Comparing Fig.9(a)(ii) with (b)(ii) (or (b)(ii)*), we show the obvious different of chaotic attractor for the slight change of f .

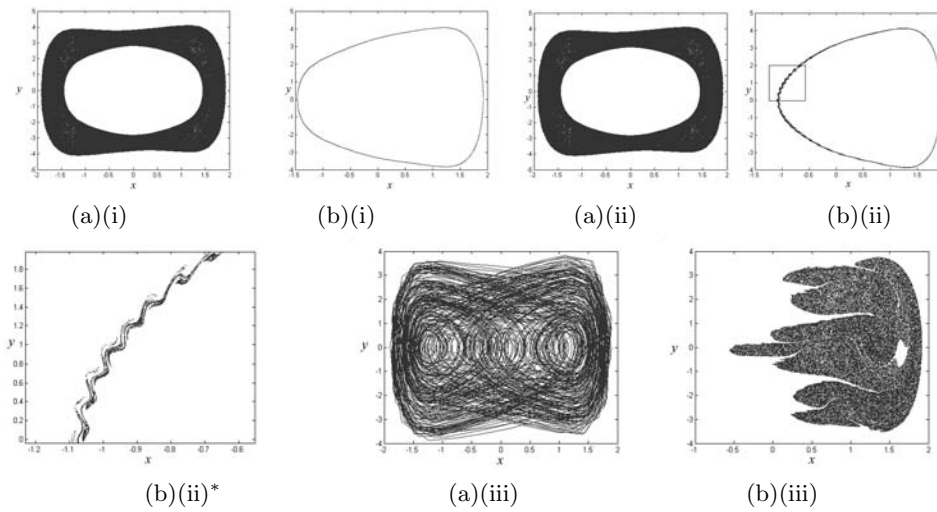


Figure 9. (a) Phase portraits of various of f in Fig.8(a), (b) Poincaré maps of (a). (i) $f = 2.05$, (ii) $f = 2.7$, (iii) $f = 3.1$. Here (ii)* is local amplification of box in (b)(ii).

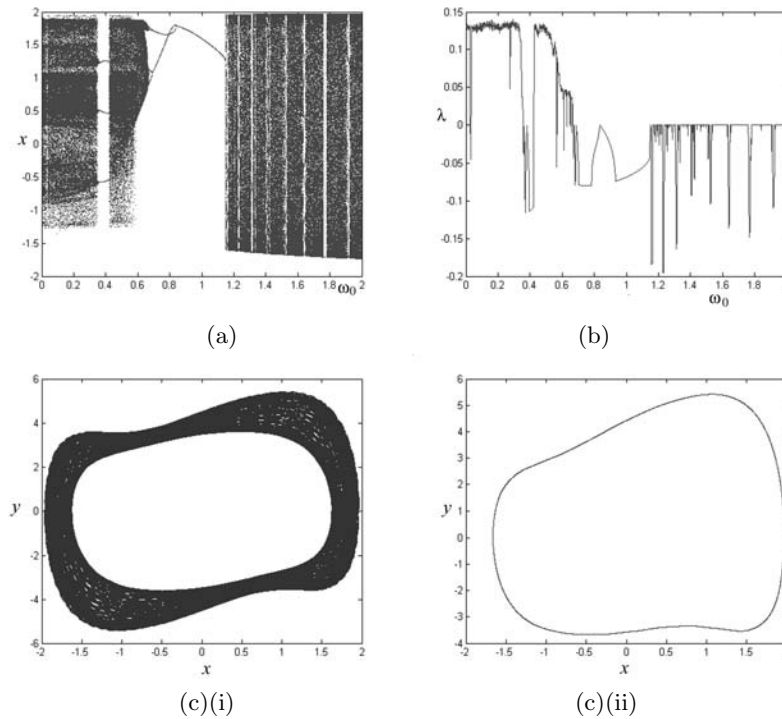


Figure 10. (a) Bifurcation diagram of system (1.1) in (ω_0, x) plane for $\beta = -3, \gamma = 2, p = 1, f = 2, \omega = 1$; (b) maximal Lyapunov exponent corresponding to (a); (c) Invariant torus for $\omega_0 = 1.45$ in (a): (c)(i) Phase portrait, (c)(ii) Poincaré map.

For case (2). The bifurcation diagram of system (1.1) in (ω_0, x) plane and the corresponding maximum Lyapunov exponents are given in Fig.10(a) and Fig.10(b). From Fig.10(a) we observe that the processes of inverse period-doubling bifurcation leading to chaos with period-3 window for $\omega_0 \in (0, 1.15)$ and there are invariant torus regions with period windows for $\omega_0 \in (1.15, 2)$. The phase portrait and Poincaré map of invariant torus at $\omega_0 = 1.45$ ($L = -0.000034$) are shown in Fig.10(c)(i) and (c)(ii).

For case (3). The bifurcation diagram of system (1.1) in (γ, x) plane and the corresponding maximum Lyapunov exponents for $\omega_0 = 1$ are given in Fig.11(a) and Fig.11(b). The local amplifications of Fig.11(a) for $\gamma \in (0.9, 1.15)$ and $\gamma \in (2.3, 2.9)$ are given in Fig.11(c) and (d), respectively. There are the onset of chaos at $\gamma \approx 0.975$ and a small chaotic region with periodic windows for $\gamma \in (0.975, 1.12)$ and a more wide period one window for $\gamma \in (1.2, 2.34)$ in Fig.11(a) and (c). We also see the interleaving occurrences of invariant torus and periodic windows (periods 19, 9, 1, 9, 15, 5) as γ increasing from 2.54 in Fig.11(d).

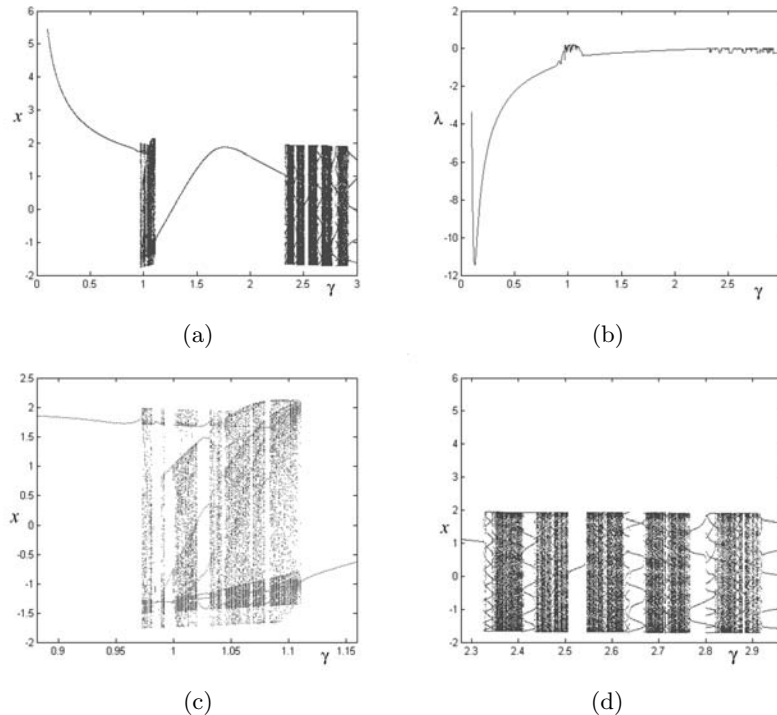


Figure 11. (a) Bifurcation diagram of system (1.1) in (γ, x) plane for $\beta = -3, \omega_0 = 1, p = 1, f = 2, \omega = 1$; (b) maximal Lyapunov exponent corresponding to (a); (c) local amplification of (a) for $0.9 < \gamma < 1.15$; (d) local amplification of (a) for $2.3 < \gamma < 2.9$.

The bifurcation diagram of system (1.1) in (γ, x) plane and corresponding maximum Lyapunov exponents for $\omega_0 = \sqrt{2}$ are given in Fig.12(a) and (b). The local amplifications of Fig.12(a) for $\gamma \in (0.65, 0.95)$ is given in Fig.12(c). We observe that a period doubling cascade to chaos as $\gamma \in (0.733, 0.765)$, a period-3 window as $\gamma \in (0.786, 0.806)$ and the symmetry-breakings of two pairs periodic orbits at

$0.859 < \gamma < 0.876$, and chaotic regions with period and quasi-periodic windows.

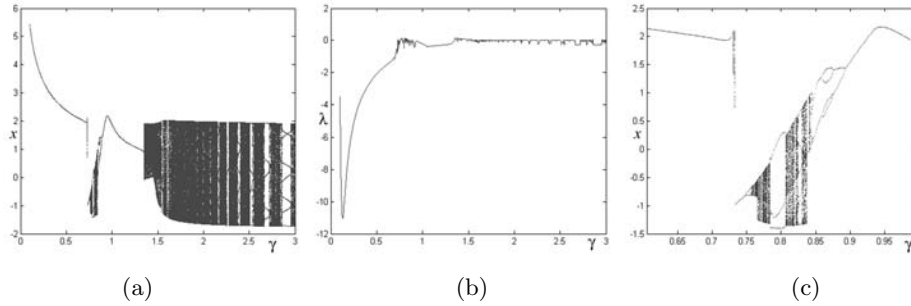


Figure 12. (a) Bifurcation diagram of system (1.1) in (γ, x) plane for $\beta = -3, \omega_0 = 1, p = 1, f = 2, \omega = 1$; (b) maximal Lyapunov exponent corresponding to (a); (c) local amplification of (a) for $0.9 < \gamma < 1.15$; (d) local amplification of (a) for $2.3 < \gamma < 2.9$.

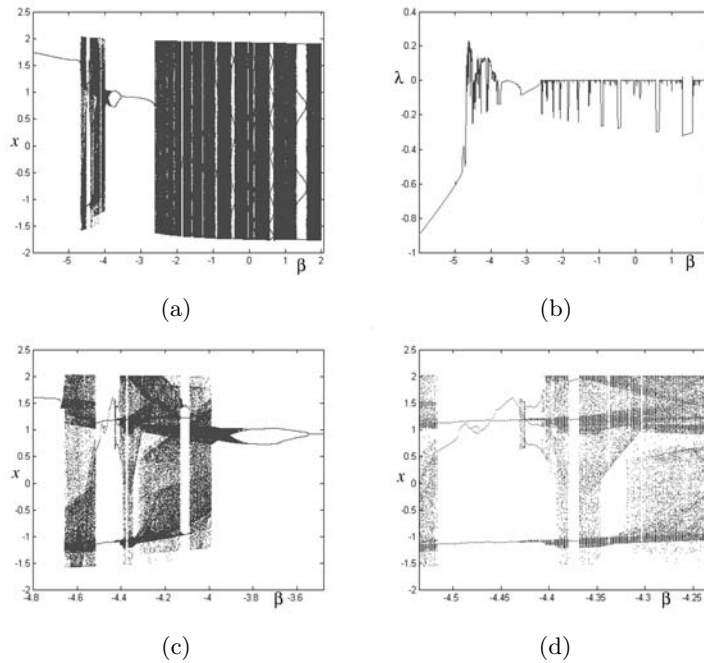


Figure 13. (a) Bifurcation diagram of system (1.1) in (β, x) plane for $\gamma = 2, \omega_0 = 1, p = 1, f = 2, \omega = 1$; (b) maximal Lyapunov exponent corresponding to (a); (c) local amplification of (a) for $-4.8 < \beta < -3.6$; (d) local amplification of (a) for $-4.5 < \beta < -4.3$.

For case (4). The bifurcation diagram of system (1.1) in (β, x) plane and corresponding maximum Lyapunov exponents for $\omega_0 = 1$ are given in Fig.13(a) and (b), and the local amplified bifurcation diagrams of Fig.13(a) for $\beta \in (-4.8, -3.6)$, and $\beta \in (-4.5, -4.25)$ are shown in Fig.13(c)-(d). The system exhibits the onset of

chaos from period-one orbit and the processes of inverse period-doubling bifurcation leading to the same chaotic region, and the symmetry-breakings of two pairs periodic orbits for $\beta \in (-4.481, -4.472)$. We also note that the invariant torus regions with periodic windows as $\beta \in (-2.631, 2)$.

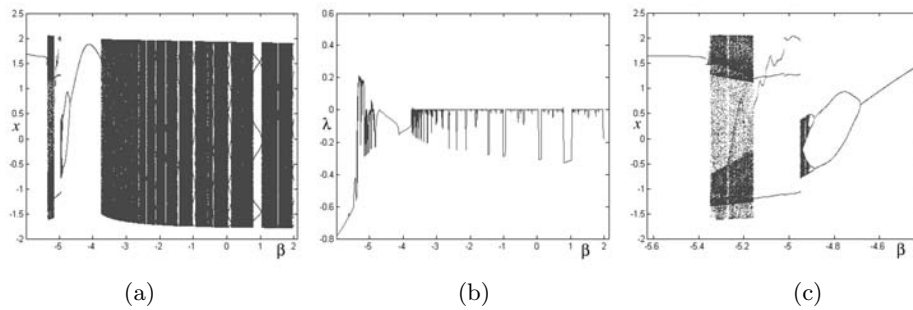


Figure 14. (a) Bifurcation diagram of system (1.1) in (β, x) plane for $\gamma = 2, \omega_0 = \sqrt{2}, p = 1, f = 2, \omega = 1$; (b) maximal Lyapunov exponent corresponding to (a); (c) local amplification of (a) for $-5.6 < \beta < -4.6$.

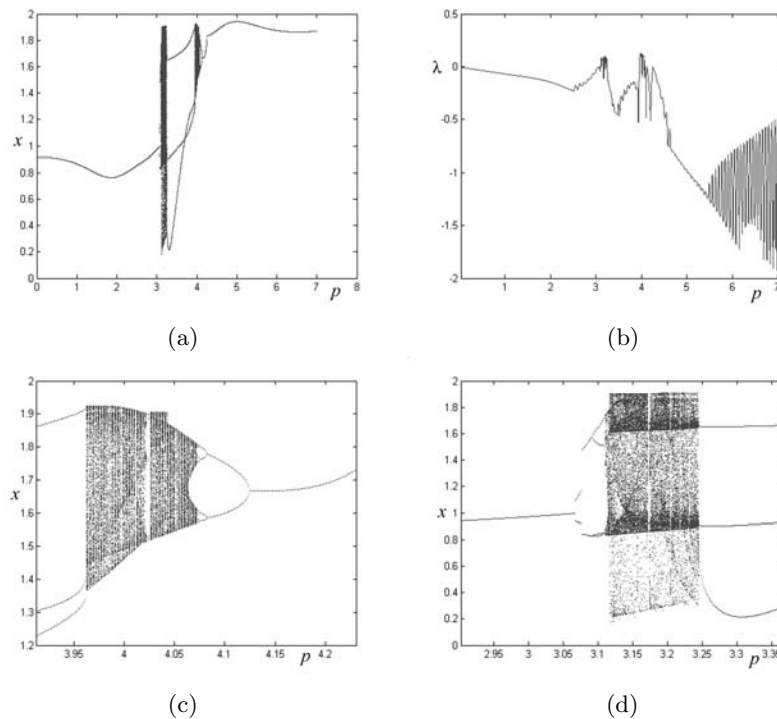


Figure 15. (a) Bifurcation diagram of system (1.1) in (p, x) plane for $\beta = -3, \gamma = 2, \omega_0 = 1, f = 2, \omega = 1$; (b) maximal Lyapunov exponent corresponding to (a); (c) local amplification of (a) for $2.95 < p < 3.35$; (d) local amplification of (a) for $3.95 < p < 4.2$.

The bifurcation diagram of system (1.1) in (β, x) plane and corresponding maximum Lyapunov exponents for $\omega_0 = \sqrt{2}$ are given in Fig.14(a) and (b), and the local amplified bifurcation diagrams of Fig.14(a) for $\beta \in (-5.6, -4.6)$ is shown in Fig.14(c). As β is decreased, we observe that the process of inverse period-doubling bifurcation leading to chaos, and the chaos suddenly disappearing at $\beta \approx -4.95$ and period-3 orbit appearing until onset of chaos at $\beta \approx -5.16$. We also show the quasi-periodic orbit regions with period motions (period-6, 7 and so on) as $\beta \in (-3.744, 2)$.

For case (5). The bifurcation diagram of system (1.1) in (p, x) plane and the corresponding maximum Lyapunov exponents for $\omega_0 = 1$ are shown in Fig.15(a) and (b), the local amplified bifurcation diagrams of Fig.15(a) for $p \in (2.95, 3.35)$ and $p \in (3.95, 4.2)$ are given in Fig.15(c) and (d), respectively. We show that the period-doubling bifurcation leading to a small chaotic region, and the inverse period-doubling bifurcation leading to another small chaotic region, and two more wide period-one regions.

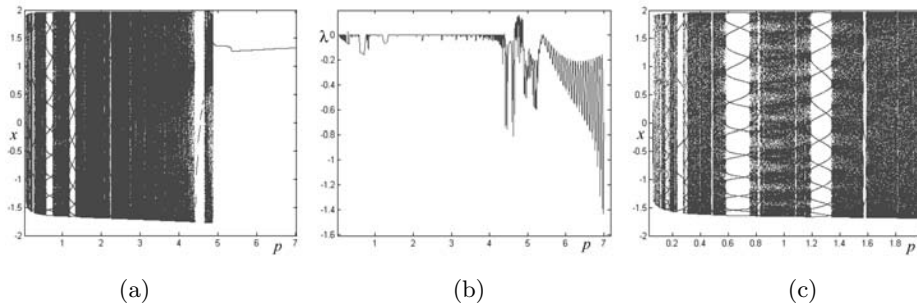


Figure 16. (a) Bifurcation diagram of system (1.1) in (p, x) plane for $\beta = -3, \gamma = 2, \omega_0 = \sqrt{2}, f = 2, \omega = 1$; (b) maximal Lyapunov exponent corresponding to (a); (c) local amplification of (a) for $0 < p < 4$.

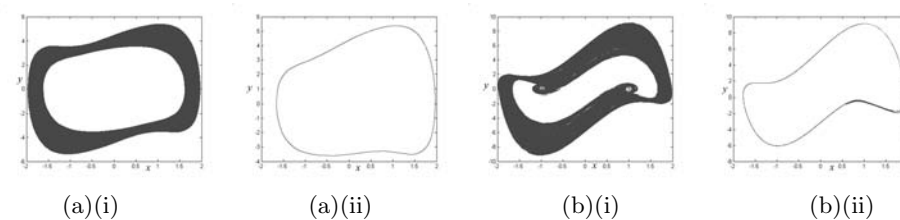


Figure 17. (a) Quasiperiodic orbit for $p = 0.5$ in Fig.16(a): (a)(i) phase portrait, (a)(ii) Poincaré map. (b) Chaotic attractor for $p = 4.75$ in Fig.16(a): (b)(i) phase portrait, (b)(ii) Poincaré map.

The bifurcation diagram of system (1.1) in (p, x) plane and corresponding maximum Lyapunov exponents for $\omega_0 = \sqrt{2}$ are shown in Fig.16(a) and (b), the local amplifications of Fig.16(a) for $p \in (0, 0.4)$ is given in Fig.16(c). There are the period-one orbit suddenly converting to quasi-periodic orbits and the chaotic region with small positive Lyapunov exponents, and complex periodic windows (periods 3, 11, 23, 11, 23, 21, 11, 19, 29, 5, 21, 39, 21 and so on) as p increasing, and they appear

alternatively, and the final chaotic region, ending in a periodic-one orbit. The quasi-periodic orbit at $f = 0.5(L = 0)$ and chaotic attractor at $f = 4.75(L = 0.110068)$ are given in Fig.17(a) and (b), respectively.

For case (6). (i) The bifurcation diagram of system (1.1) in (ω, x) plane and maximum Lyapunov exponents for $\omega_0 = \sqrt{2}$ are shown in Fig.18(a) and (b). The local amplified bifurcation diagram of Fig.18(a) for $\omega \in (0, 0.4)$ and $\omega \in (0.136, 0.15)$ are given in Fig.18(c) and (d). The system (1.1) exhibits the quasi-periodic route to chaos in Fig.18(c), and another two routes to chaos: period-doubling bifurcation to chaos, and inverse period-doubling bifurcation to chaos in Fig.18(a) and (d). We also show that the interleaving occurrence of chaotic behaviors and quasi-periodic, and the chaotic regions with period-windows, and the jumping behaviors of periodic orbit and the symmetry-breaking of one pair period-orbit, and the chaos ending in a periodic orbit in Fig.18(a)-(d). The phase portrait of quasi-periodic orbits is given in Fig.18(e).

Remark. The bifurcation diagram in (ω, x) plane and maximum Lyapunov exponents for $\omega = 1$ (in case (6)) are similar to the Fig.18(a) and (b), so omit the Figures here.

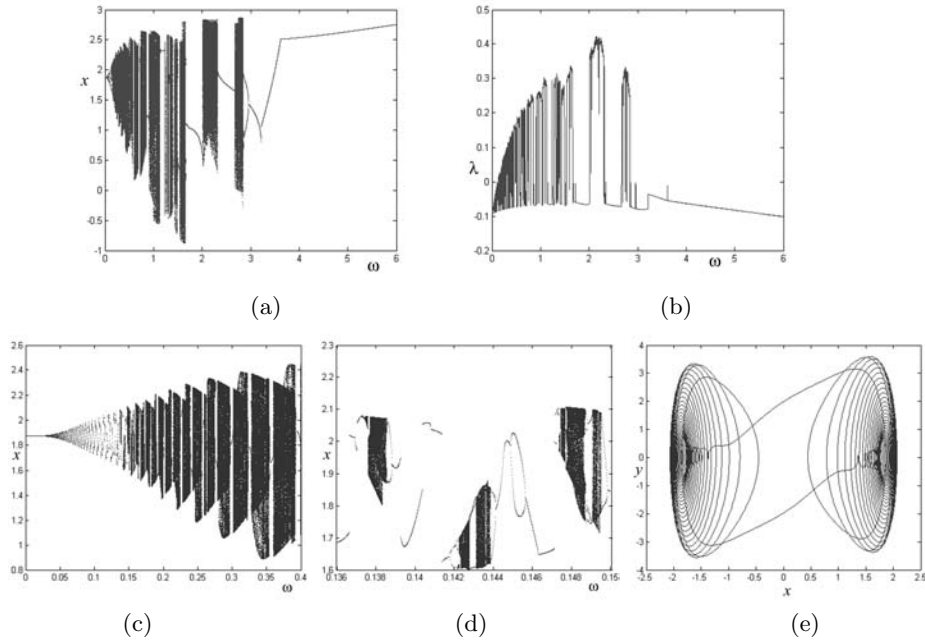


Figure 18. (a) Bifurcation diagram of system (1.1) in (ω, x) plane for $\beta = -3, \gamma = 2, \omega_0 = \sqrt{2}, p = 0.1, f = 30$; (b) maximal Lyapunov exponent corresponding to (a); (c) local amplification of (a) for $0 < \omega < 0.4$; (d) local amplification of (a) for $0.136 < \omega < 0.15$; (e) phase portrait of quasi-periodic orbits for $\omega = 0.1$ of (a).

(ii) The bifurcation diagram of system (1.1) in (ω, x) plane and the corresponding maximum Lyapunov exponents for $\omega_0 = 1$, and $f = 2$ are shown in Fig.19(a) and (b), the local amplified bifurcation diagram of (a) for $\omega \in (1.3, 1.5)$ is given in (c). There are the chaotic regions with period windows (period 3, 7 and so on), and the chaos suddenly converting to periodic one orbit.

(iii) The bifurcation diagram of system (1.1) in (ω, x) plane for $\beta = 0.2, \gamma = 1, \omega_0 = \sqrt{2}, p = 3$ and $f = 0.5$ and maximum Lyapunov exponents are shown in Fig.20(a) and(b), where we show that the maximum Lyapunov exponents are equal or approximate to zero except for a small interval of ω . The system (1.1) therefore presents fundamentally the quasiperiodic behaviors and chaotic behaviors except for a small period-window. The phase portraits of the chaotic behavior and quasiperiodic behavior for $\omega = 4.693$ ($L = 0.00039129$) and $\omega = 5.95$ ($L = -0.0020617$) are given in Fig.20(c) and (d), respectively.

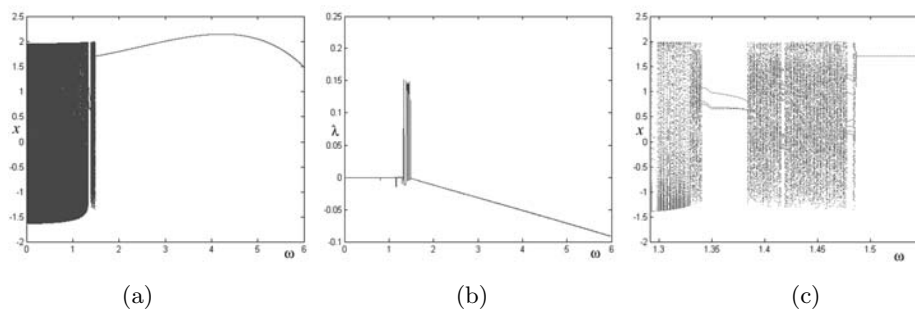


Figure 19. (a) Bifurcation diagram of system (1.1) in (ω, x) plane for $\beta = -3, \gamma = 2, \omega_0 = 1, p = 0.1, f = 2$; (b) maximal Lyapunov exponent corresponding to (a); (c) local amplification of (a) for $1.3 < \omega < 1.5$.

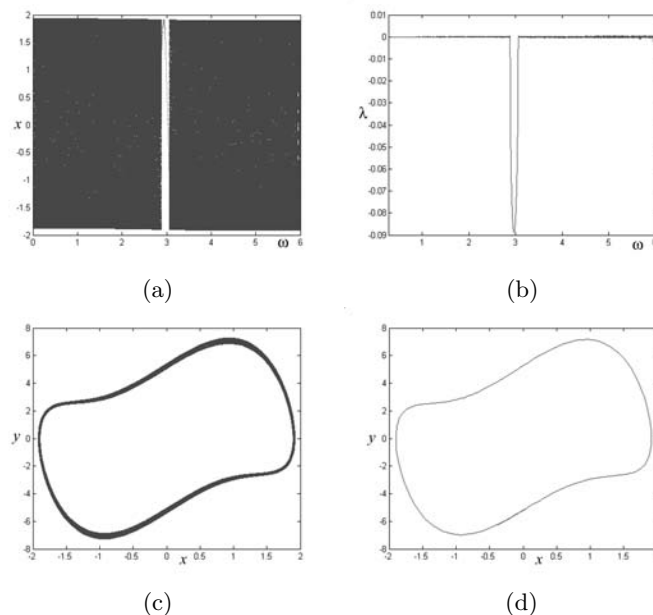


Figure 20. (a) Bifurcation diagram of system (1.1) in (ω, x) plane for $\beta = 0.2, \gamma = 1, \omega_0 = \sqrt{2}, p = 3, f = 0.5$; (b) maximal Lyapunov exponent corresponding to (a); (c) Poincaré map of chaotic attractor for $\omega = 4.693$ of (a); (d) Poincaré map of quasiperiodic orbit for $\omega = 5.95$ of (a).

9. Remark

In this paper and previously paper [7], we have investigated the dynamical behaviors of Duffing-Van der Pol equation with an external forcing and two external forcings, respectively. We give the conditions of existences and bifurcations for harmonic, subharmonics, superharmonic and chaos for the system with one forcing in the paper. And we give the threshold values of existence of chaotic motion under the periodic perturbation for original system and under quasiperiodic perturbation for averaged system for the system with two external forcings, but haven't to give the condition of various subharmonics in [7]. Moreover, comparing Fig.10, Fig.15, Fig.18, Fig.21, Fig.24, Fig.25 in [7] with Fig.6, Fig.10, Fig.11, Fig.13, Fig.15, Fig.18 in the paper, respectively, we shown the dynamical behaviors of one external forcing are different from that of two external forcings. In particular, there are the more small chaotic regions (Lyapunov exponent approximating to zero and small size) with a great abundance of periodic windows, and the system can be leave chaotic region to periodic motion by adjusting the parameters p, β, γ, f and ω , which can be considered as a control strategy for the system with one external forcing. But there are the more large chaotic regions (larger Lyapunov exponent and wide region) with quasi-periodic, periodic widows, and the system can leave chaotic region to periodic motion by adjusting the parameter f_2 and there are always the chaotic behavior or quasi-periodic behavior as adjusting other parameters for two external forcings. These results are useful for understanding dynamical behaviors for the Duffing-Van der Pol system.

References

- [1] K. Alligood, T. Saue and J. Yorke, *Chaos-An introduction to dynamical systems*, Springer, 1996.
- [2] J. Guckenheimer, K. Hoffman and W. Weckesser, *The forced Van der Pol equation. I. The slow flow and its bifurcations*, SIAM. J. Appl. Dyn. Syst., 2(2003), 1-35.
- [3] J. Guckenheimer, and P. Holmes, *Dynamical systems and bifurcations of vector fields*, Springer-Verlag, New York, 1997.
- [4] J. Hale and H. Kocak, *Dynamics and Bifurcations*, Springer-Verlag, 1991.
- [5] C. Holmes and P. Holmes, *Second order averaging and bifurcations to subharmonics in Duffing's equation*, Journal of Sound and Vibration, 78(1981), 161-174.
- [6] Z. Jing and R. Wang, *Chaos in Duffing system with two external forcing*, Chaos, Solitons and Fractals, 23(2005), 399-411.
- [7] J. Jing, Z. Yang and T. Jiang, *Complex dynamics in Duffing-Van der Pol equation*, Chaos, Solitons and Fracals, 27(2006), 722-747.
- [8] F. Kakmeni, S. Bowvng, C. Tchawoua and E. Kaptouom, *Strange attractors an chaos control in a Duffing-Van der oscillator with two external periodic forces*, J. Sound Viber., 227(2004), 783-799.
- [9] Y. Kao and C. Wang, *Analog study of bifurcation structures in a Van der Pol oscillator with a nonlinear restoring force*, Phys. Rev. E, 48(1993), 2514-2520.

- [10] T. Kapitaniak, *Analytical condition for chaotic behavior of the Duffing oscillation*, Phys. Lett. A, 144(1990), 322-324.
- [11] H. Kielhöfer, *Bifurcation theory-An introduction with applications to PDEs*, Springer, 2004.
- [12] Y. Kuznetsov, *Elements of applied bifurcation theory, (3rd Edition)*, Springer, 2004.
- [13] M. Lakshmanan and M. Murali, *Chaos in nonlinear oscillations*, World Scientific, 1996.
- [14] A. Leung and Q. Zhang, *Complex normal form for strongly non-linear vibration systems exemplified by Duffing-Van der Pol equation*. J. Sound Viber., 213(1998), 907-914.
- [15] Y. Liang and N. Namachchuraya, *P-bifurcation in the noise Duffing-Van der Pol equation*, Stochastic Dynamics, by H. Crauel, and M. Gundlach, Springer, New York, 1999.
- [16] F. Moon, *Chaotic and fractal dynamics-An introduction for applied scientists and engineers*, A Wiley-Interscience Pub., 1992.
- [17] T. Mullin, *The nature of chaos*. Clarendon Press, Oxford, 1993.
- [18] H. Nagashima and Y. Baba, *Introduction to chaos*, Institute of Physics Publishing, Bristol and Philadelphia, 1992.
- [19] N. Nawachchivaga, R. Sowers and L. Vedula, *Non-standard reduction of nise Duffing-Van der Pol equation*, Dyn Syst., 16(2001), 223-245.
- [20] U. Parlitz U and W. Lauterborn W., *Period-doubling cascades and Peril's staircases of the Driven Van der Pol oscillator*, Phys. Rev. A, 36(1987), 1482-1434.
- [21] J. Sanders and F. Verhulst, *Averaging Methods in Nonlinear Dynamical Systems*, Springer-Verlag, New York, 1985.
- [22] M. Wakako, M. Chieko, H. Koi-ichi and H. Yoshi, *Integrable Duffing's maps and solutions of the Duffing equation*, Chaos, Solitons and Fractals, 15(2003), 425-443.
- [23] S. Wiggins, *Introduction to applied nonlinear dynamical System and chaos*, Springer-Verlag, New York, 1990.
- [24] K. Yagasaki, *Second-order averaging and Melnikov analyses for forced nonlinear oscillators*, Journal of Sound Viber., 190(1996), 587-609.
- [25] K. Yagasaki, *Homoclinic tangels, phase locking, chaos in a two frequency perturbation of Duffing's equation*, J. Nonlinear Sci., 9(1999), 131-148.